EVALUATION OF COLLECTION EFFICIENCY METHODS FOR ICING ANALISYS

Rafael A. da Silveira
Departamento de Engenharia Mecânica – UFSC, Caixa Postal 476, 88040-000 Florianópolis SC, Brasil.
silveira@sinmec.ufsc.br

Clovis R. Maliska
Departamento de Engenharia Mecânica – UFSC, Caixa Postal 476, 88040-000 Florianópolis SC, Brasil.
maliska@sinmec.ufsc.br

Diego A. Estivam
Departamento de Engenharia Mecânica – UFSC, Caixa Postal 476, 88040-000 Florianópolis SC, Brasil.
estivam@sinmec.ufsc.br

Rafael Mendes
Departamento de Engenharia Mecânica – UFSC, Caixa Postal 476, 88040-000 Florianópolis SC, Brasil.
rmendes@sinmec.ufsc.br

Abstract. *Collection efficiency is used to measure the water flux impinging on a surface of an aircraft when it flies through a cloud under icing conditions. It is defined as the ratio of surface to free-stream water mass fluxes. There are two classes of methods for its calculation: Lagrangean and Eulerian methods. Lagrangean methods consist of solving the water droplets trajectory equations and computing the impingement locations. Eulerian methods handle with transport equations for momentum and phase volume fraction for both water and air. In general, the air flow is computed by a Navier-Stokes or an Euler solver and then the water momentum and volume fraction equations are solved considering the momentum transfer between the phases. A new approach, proposed in this work, is solving the air and water phases simultaneously using a multiphase formulation, which accounts for the water droplets influence in the air flow and other physical effects. This can be useful for large droplets simulation. Eulerian methods are especially useful for complex geometries, since it is difficult to compute the droplet impact position using the lagrangean formulation in those geometries. This paper describes these methods and compares the results with some experimental and numerical data available in the literature.*

Keywords*: Collection efficiency, Eulerian method, Lagrangean method, aircraft ice accretion.*

1. Introduction

When an aircraft flies through a cloud, super-cooled water droplets impinge on the surfaces and freeze, forming an ice layer that changes the geometry and affecting the aerodynamic characteristics of the plane. Wings and nacelles inlet are the most critical surfaces affected by this phenomenon. Wings have their lift reduced and drag increased, while the efficiency of the engines is prejudiced by the ice accumulation on the inlet of the nacelles. Control surfaces, as flaps and ailerons, empennages and the windshield are also affected.

With the purpose of designing anti-icing systems, physical models for ice accretion have been developed since 1950's and computational fluid dynamics has been used for solving these models. Basically, an icing model consists of solving the external flow equation and computing the water impinging flux on the surface. Heat and mass balances are carried out to find the freezing flux and then the ice thickness can be calculated. More details about thermodynamic models can be encountered in Wright (1995), Bourgault et all (2000a), Hedde and Guffond (1995), Morency et all (1999) and Silveira (2001).

A precise water impinging flux is a very important factor for the icing analysis, therefore, a special attention need to be given for the collection efficiency calculation. Lagrangean methods have been used since the first ice accretion codes. Lewice, from the NASA Glenn Research Center is the most famous code for ice accretion simulation and uses this methodology, as can be seen in Wright (1995). In this code, a distribution of droplets of different sizes can be considered for the analysis and very good agreement is achieved for the geometries considered. Other methods also use the Lagrangean methodology like CANICE and ONERA icing codes (see Morency et all (1999) and Hedde and Guffond (1995) respectively). A more recent work by Bourgault et all (1999) deals with an Eulerian methodology to account for water droplets impingement and the model is implemented in the FENSAP-ICE code. Such methodology has been successfully used for collection efficiency calculation in complex 3D geometries, like nacelles and air intakes of helicopters.

This paper compares the results of three methods for calculating the collection efficiency. The theory behind these methodologies is described in the following sections. The advantages and applicability of each one are also discussed.

2. Lagrangean formulation

In the Lagrangean formulation, the trajectory of each particle is computed based on a force balance, according to Fig.1. A water droplet is considered to be rigid sphere that do not affect the flow but undergoes aerodynamic drag.

Besides, the gravity force can be ignored for small droplet diameters, like in typical icing conditions. If one carries out the force balance for a two-dimensional case, it results in

$$m\frac{d^2x_p}{dt^2} = -D\cos\gamma \tag{1}$$

$$m\frac{d^2y_p}{dt^2} = -D\sin\gamma \tag{2}$$

where γ is the angle between the local droplet and air velocities and is written as

$$\gamma = \tan^{-1}\left(\frac{v_p - v_a}{u_p - u_a}\right) \tag{3}$$

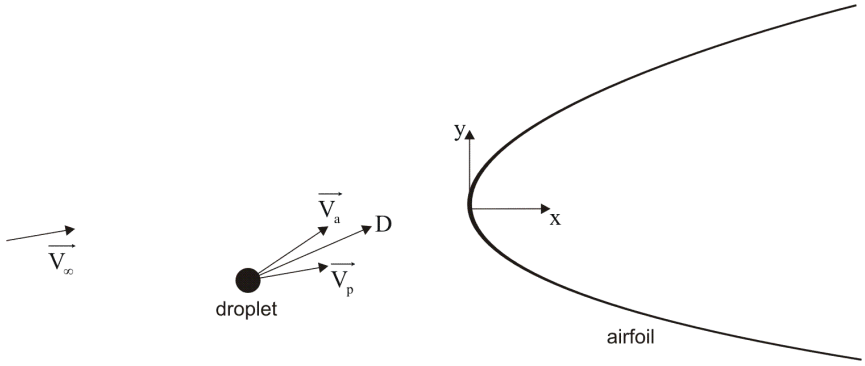

Figure 1: Force balance on a droplet

The drag force is expressed in function of a drag coefficient developed for spheres. In White (1991), the following expression can be found

$$c_d = \frac{24}{Re_d} + \frac{6}{1+Re_d^{0.5}} + 0.4 \tag{4}$$

where $Re_d = Vd/\nu$ is the droplet Reynolds number and d is the droplet diameter. The relative velocity V is given by

$$V = \sqrt{(u_p - u_a)^2 + (v_p - v_a)^2} \tag{5}$$

Another expression for the drag coefficient can be found in Bourgault et all (1999) and is known as the Shiller Naumann coefficient, given by

$$c_d = \frac{24}{Re_d}\left(1 + 0.15Re_d^{0.687}\right) \tag{6}$$

for $Re_d \leq 1000$ and $c_d = 0.4$ for $Re_d > 1000$.

The drag force is then written as

$$D = c_d\rho_a\frac{V^2}{2}A_p \tag{7}$$

Note that a numerical solution is required since the drag force depend on the droplet velocity that depends on the local air velocity.

The droplets are “released” at a sufficiently distant position from the body so that the air flow is not affected. The trajectory equations are solved until it intercepts the surface. The impingement limits are computed by an iterative process. For the upper limit, a trajectory hitting the body and the next one above which does not hit the surface are chosen. A trajectory lying halfway between these two is computed. If it misses the body, it is considered as the new

trajectory which does hit the surface. If it impinges the body it is the new hitting trajectory. This procedure is repeated until the gap of the initial position of the two droplets is smaller then a specified value. The same approach is applied for the lower limit

The initial positions and the respective impingement positions of the droplets define a function $y_0(s)$, according to Fig.2. Since the collection efficiency is defined as the ratio of the surface and the free-stream water fluxes per unit of area, this coefficient can be written as

$$\beta = \frac{dy_0}{ds} \tag{8}$$

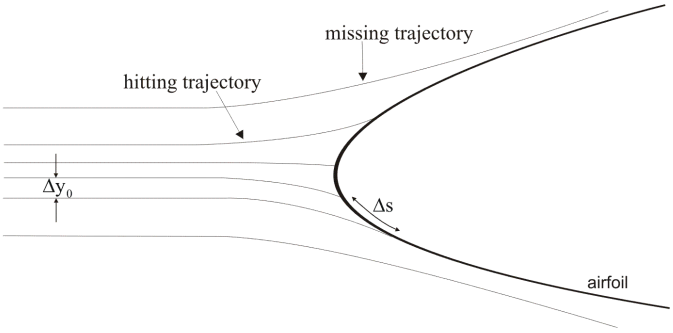

Figure 2: 2D Collection efficiency calculation

For 3D cases, a similar trajectory equation for the z-component is added to the system. The collection efficiency is computed defining a function $A_0(A_m)$, where A_0 is the area formed by the initial position of four droplets and A_m is the area formed by their respective impingement positions at the body, as shows the Fig.3 extracted from Kind et all 1998. So, one can determine β by differentiating A_0 with respect to A_m.

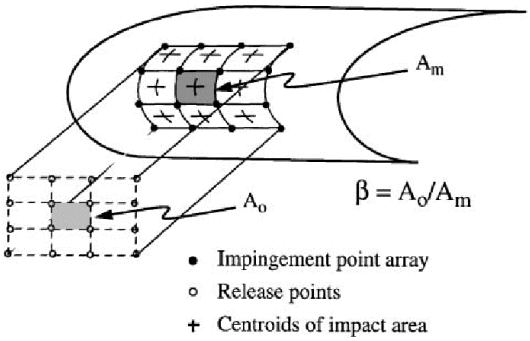

Figure 3: Three-dimensional approach for collection efficiency (Kind et all, 1998)

This approach can be applied for 3D simple geometries like wings or fuselage, but it becomes problematic when more complex geometries are analyzed, like a nacelle or, in a critical case of an entire aircraft, since it is too difficult predict exact impingement positions in such cases. Another problem is related to the air flow solver that is used for the calculations. In Silveira (2001), Silveira and Maliska (2001) and Wright (1995), the air flow is computed by the panel method (an inviscid solution). This approach does not require a grid for solving the equations, although it can be used. The air velocity is computed for all the droplet positions along its trajectory and a large amount of computation can be required. This problem could be avoided by using a grid-based flow solution like in Hedde and Guffond (1995) and Morency et all (1999). However, problems related to interpolation of the velocities arise, since the air velocity is known only in the grid nodes (or the center of the cells, depending on the formulation). The process of searching the cell where the droplet is located may be computationally very expensive when the grid is large, especially for tree-dimensional geometries.

3. Eulerian approach

The Eulerian approach could be considered a more general formulation for calculating collection efficiency. It consists of solving transport equations for momentum and phase volume fraction. A formulation of this type was proposed by Bourgault et all (1999) and implemented in the code FENSAP-ICE. In this work, it is assumed that the water droplets do not affect the air flow and the water equations are solved independently. This approach will be referred along the text as the "passive scalar transport method", since water velocity and volume fraction are just "convected" by the air flow.

In this paper it is presented another alternative for computing the air-water flow. It uses the two-fluid model extensively used for the solution of multi-phase flow problems and the scheme used is the one implemented in the commercial software CFX 5.5 (©AEA Technology plc.), with appropriate boundary conditions and multiphase options available in the program. In these methods, both air and water are treated as a continuum fluid, which is a characteristic of the multiphase formulations. Both methodologies are reported in the following sections.

3.1 Passive scalar transport approach

The model proposed by Bourgault et all (1999) solves the disperse phase (water droplets) independent of the continuous phase (air). The air flow is computed by an Euler or a Navier-Stokes solver using the finite element method and the turbulence model of Spallart-Almaras. The governing equations for the disperse phase consist of one equation for conservation of the water volume fraction and one momentum equation for each component of the water velocity. The volume fraction is the fraction of a control volume occupied by a phase. It can be also defined as the phase concentration (liquid water content in the case of water droplets in the air) divided by its density (water density).

Therefore, the governing equations for the water are

$$\frac{\partial \alpha}{\partial t} + \vec{\nabla} \cdot (\alpha \vec{u}) = 0 \tag{9}$$

$$\frac{\partial (\alpha \vec{u})}{\partial t} + \vec{\nabla} (\alpha \vec{u} \vec{u}) = \frac{c_d \, Re_d}{24K} \alpha (\vec{u}_a - \vec{u}) + \left(1 - \frac{\rho_a}{\rho}\right) \frac{\alpha}{Fr^2} \vec{g} \tag{10}$$

where α is the non-dimensional volume fraction of water (divided by $\alpha_\infty = LWC/\rho$), $\vec{u}$ and $\vec{u}_a$ are the non-dimensional water and air velocity, respectively, (divided by U_∞), ρ and ρ_a are the water and air densities, respectively, and K is an inertia parameter defined as

$$K = \frac{\rho d^2 U_\infty}{18 L \mu} \tag{11}$$

being L a characteristic length (the airfoil cord length, for example), d is the droplets mean diameter and μ is the water viscosity. The Froude number is defined as

$$Fr = \frac{U_\infty}{\sqrt{Lg}} \tag{12}$$

The drag coefficient and Reynolds number are defined in the same way as written previously for the Lagrangean formulation. In this theory, the Shiller Naumann coefficient is used for drag.

It can be noted in the RHS of the momentum equation that the model considers drag (first term), buoyancy (second term) and gravity (third one) forces acting on the droplets. In general, the buoyancy effects can be neglected for typical icing conditions, since $\rho >> \rho_a$, as well as the gravity term, by considering that the Froude number is of the order of U_∞.

The same grid used for the air flow solution is used for the numerical solution of the water equations. Special attention must be given to the boundary conditions. One can define three types of physical boundaries in a numerical solution of an aerodynamic problem, i.e. an *Inlet*, an *Outlet* and a *Wall* conditions, as in Fig.4 for a 2D typical aerodynamic "C-domain".

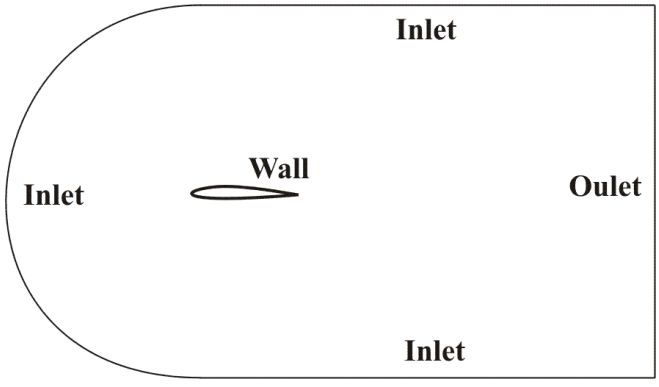

Figure 4: Typical "C-Domain" for airfoil simulation

The *Inlet* boundary is a location that is not affected by the presence of the body. Then, one imposes free-stream conditions for water velocity (equal to free-stream air velocity) and water volume fraction in these boundaries. In the *Outlet* boundary, the fluid is assumed to recover its free-stream pressure, so that this pressure can be set for this boundary. The velocity is assumed not changing and a condition of zero velocity derivative is imposed.

The *Wall* boundary is the most complex to deal with, since one wants to compute "impact" positions on the surface. In the real problem, the water which impinges the surface can be seen as "entering" the wall. To simulate such effect, the wall is treated as an *Outlet* boundary condition with no pressure imposed there. However, *Outlet* boundary condition may allow flow from the wall to the computational domain (which would be unphysical). To apply zero velocity derivative is not sufficient to represent the correct physical behavior. The procedure adopted here is to compute the normal component of the water velocity vector at the surface. If it "leaves" the wall it set to zero, otherwise it is the correct and it represents the impinging velocity at the wall.

The collection efficiency coefficient in each location of the body is recovered by the following expression

$$\beta = -\alpha_s \vec{u}_s \cdot \vec{n} \tag{13}$$

where α_s and $\vec{u}_s$ are the surface values of the water velocity and volume fraction and $\vec{n}$ is the normal vector outward the wall boundary.

This method has been used successfully to predict collection efficiency for complex geometries, like nacelles, air intake of helicopters, multi-element airfoils and fuselages for some typical icing conditions. Nevertheless, this model has never been tested for larger droplets influence in the turbulence production, for heat transfer due to friction on the surface, for possible evaporation (mass transfer) of the droplets and other non-typical situations.

A multiphase formulation, like the model implemented in the commercial software CFX 5.5 (©AEA Technology plc.) can be useful for trying to represent these effects. In the following section, is presented a brief description of the mathematical model implemented in the software cited above.

3.1 Full multiphase formulation

The purpose of this section is describing the mathematical model of the multiphase flow solver of the CFX 5.5 (©AEA Technology plc.) in order to apply it for the collection efficiency calculation. The CFX's multiphase flow solver covers several physical situations such as gas-solid flow, combustion, bubbles flow, etc. several models for interphase transfer of heat, mass and momentum transfer, besides turbulence are available.

In the multiphase model the governing equations of conservation of mass, momentum and energy are written for all the phases and averaged by the phase volume fraction. Turbulence models can be applied for any phase or for all of them.

Next, the system of equations required for the calculation of the water volume fraction and impingement velocities is described. The complete description of multiphase model is available in AEA Tech (2001).

For the phase i (i = a for air and i = w for water), the continuity equation is written as

$$\frac{\partial(\alpha_i \rho_i)}{\partial t} + \vec{\nabla} \cdot \left(\alpha_i \rho_i \vec{U}_i\right) = 0 \tag{14}$$

where α_i, ρ_i and $\vec{U}_i$ are the volume fraction, density and velocity of the phase i, respectively. The momentum equations can be expressed in a compact form as

$$\frac{\partial\left(\alpha_i \rho_i \vec{U}_i\right)}{\partial t} + \vec{\nabla} \cdot \left(\alpha_i \rho_i \vec{U}_i \vec{U}_i\right) = -\alpha_i \vec{\nabla} p_i + \vec{\nabla} \cdot \left\{\alpha_i \mu_i \left[\vec{\nabla}\vec{U}_i + \left(\vec{\nabla}\vec{U}_i\right)^T\right]\right\} + S_i + M_i \tag{15}$$

where p_i and μ_i are the pressure and viscosity of the phase i. S_i describes momentum sources due to external forces acting on that phase and M_i represents the interfacial forces acting on phase i due to the presence of the other phase. This two source term will be discussed later.

The closure of the system of hydrodynamic requires the following constraint relations:

$$\alpha_a + \alpha_w = 1 \tag{16}$$

$$p_a = p_w = p \tag{17}$$

Interphase momentum transfer is due to the interfacial force acting on a phase i due to he presence of other phases. In the case of two phases, the interfacial forces are equal and opposite (for air and water, $M_a = - M_w$). The total interfacial force is a contribution of several physical mechanisms as the drag, lift, wall lubrication, virtual mass and

turbulence dissipation forces. All of the models are implemented in the software, but only drag will be considered to be important at this point.

The drag force exerted by the droplets on the air flow is given by the general form

$$\vec{D}_a = c_{aw}^{(d)}\left(\vec{U}_w - \vec{U}_a\right) \tag{18}$$

Total drag is more conveniently expressed as function of the dimensionless drag coefficient as

$$c_d = \frac{D}{\frac{1}{2}\rho_a\left(U_a - U_w\right)^2 A_p} \tag{19}$$

where A_p is the projected area of the droplet. After some algebraic manipulation, the drag force for the air due to the presence of water droplets is written as

$$\vec{D}_a = \frac{3}{4}\frac{c_d}{d_w} r_w \rho_a \left|\vec{U}_w - \vec{U}_a\right|\left(\vec{U}_w - \vec{U}_a\right) \tag{20}$$

being r_w and d_w the radius and diameter of the droplets, respectively. In the case of spherical particles, $r_w / d_w = 1/2$.

Drag coefficient is defined depending on the kind of particles that is being considered. Correlations for non-spherical, solid and liquid particles, for dense and dilute regimes are available. For the icing analysis, only spherical droplets will be considered and the Shiller Naumann coefficient is used, as described in early sections of this paper.

All the available turbulence models for single phase can be applied for the multiphase flow. For example, the k-ε equations are written as

$$\frac{\partial\left(\alpha_i \rho_i k_i\right)}{\partial t} + \vec{\nabla}\cdot\left(\alpha_i\left(\rho_i \vec{U}_i k_i - \left(\mu_i + \frac{\mu_{ti}}{\sigma_k}\right)\vec{\nabla} k_i\right)\right) = \alpha_i\left(P_i - \rho_i \varepsilon_i\right) \tag{21}$$

$$\frac{\partial\left(\alpha_i \rho_i \varepsilon_i\right)}{\partial t} + \vec{\nabla}\cdot\left(\alpha_i\left(\rho_i \vec{U}_i \varepsilon_i - \left(\mu_i + \frac{\mu_{ti}}{\sigma_\varepsilon}\right)\vec{\nabla} \varepsilon_i\right)\right) = \alpha_i \frac{\varepsilon_i}{k_i}\left(C_{\varepsilon_1} P_i - C_{\varepsilon_2}\rho_i \varepsilon_i\right) \tag{22}$$

where the all the terms appearing in the equations are exactly the same as the traditional k-ε model and can be easily found in the literature.

The main option of the software is the Particle Induced Turbulence Model. This model is very useful for large droplets, since larger particles increase the turbulence production in the continuum phase due to formation of wakes behind them. In this case, the eddy viscosity is modified by adding a particle induced eddy viscosity, in the form

$$\mu_{tc} = \mu_{ts} + \mu_{tp} \tag{23}$$

where μ_{tc} is the corrected eddy viscosity, μ_{ts} is the original shear induced eddy viscosity and μ_{tp} is the particle induced eddy viscosity which is given by

$$\mu_{tp} = C_{\mu P}\rho_c r_d d_p \left|\vec{U}_d - \vec{U}_c\right| \tag{24}$$

where the sub indexes c e d indicate continuum and dispersed phases respectively and $C_{\mu P}$ is a constant.

The boundary conditions are treated in the same way as for the scalar passive formulation, already described. Both phases require the same kind of boundary conditions, except for the wall boundary where a special boundary condition, named “degassing condition” must be applied. This condition, as already stated, consists in consider the wall as an outlet for the dispersed phase while the continuous phase “sees” this boundary as a free-slip wall and does not leave the domain.

Unfortunately, CFX does not support a boundary condition where the wall can be a no-slip boundary for the continuum phase and an *Outlet* for the dispersed phase. It is hopped that such option can be implemented in the software. However, it was shown in early works that viscous and inviscid air flow solutions produce quite close results.

The collection efficiency can be recovered from the water volume fraction and impingement velocities, taking into account that the variables are not non-dimensional form, as it happens in the passive scalar formulation. Thus, one can compute the coefficient as

$$\beta = -\frac{\alpha \vec{V} \cdot \vec{n}}{\alpha_\infty V_\infty} \tag{25}$$

Although many possibilities for turbulence models may exist, it is recommended to use the k-ε model for the continuum phase and a zero-equation model for the dispersed phase in order to achieve a good convergence and stability of the numerical solution.

The interphase heat transfer can be neglected for collection efficiency calculation purposes, but the authors consider a very important improvement to be included in the icing prediction codes. A crucial point is that all icing codes assume that the water droplets impinge the surface at the same free-stream temperature. In fact, the viscous heating produced by the air flow rises the fluids temperature by several degrees near the body and this energy must be transferred to the droplets. Since this topic is not on the scope of this work, the interphase heat transfer will be not described in this paper.

Since this paper presents the first developments in using this approach, it has not been yet applied for complex geometries. Due to the lack of experimental data available in the literature to validate collection efficiency computations, the multiphase approach has been applied for single airfoils and the results are presented in the next section.

The system of hydrodynamic equations is discretized using the control volume finite element method (CVFEM), which is a control volume approach for non-structured grids that solves the linear system simultaneously. Another matrix of coefficients is generated for the additional variables, such as the turbulence and energy equations.

4. Results and discussion

In this section it is presented the results for the Lagrangean and multiphase simulations for the flow around a NACA0012 airfoil and a cylinder. The Lagrangean approach is the one implemented in Silveira (2001) and the multiphase flow is computed using the CFX 5.5 software (©AEA Technology plc.). The predicted results are compared with experimental results and predicted results from other codes available in the literature.

The first case is a flow around a NACA0012 airfoil with 0.9144m of cord. The free-stream flow velocity is 44.39 m/s and the angle of attack is 0º. The LWC is 0.78 g/m^3, the free-stream temperature is 265.5 K and the median diameter of the droplets is 20 µm. The collection efficiency is compared with experimental results presented in Morency et all (1999) and it is shown in Fig. 5. The data is a log-normal distribution fitting the original wind tunnel data. The plot also shows the data obtained from Silveira (2001) and a result obtained with the code Lewice (Wright, 1995) using a droplet diameter distribution. It can be seen that a good agreement is achieved in respect to experimental data. The impingement limits is larger for the Lewice profile due to the presence of droplets with diameter greater than the average value used in the other cases.

The second case is the flow around a cylinder of radius = 0.1016 m. Free-stream velocity is 80 m/s, ambient temperature of 285.15 K, with the droplets average diameter of 16 µm and LWC = 0.55 g/m^3. Results are compared with the experimental range and a solution using the program FENSAP, both available in Bourgault et all (2000b). The validation for the cylinder case is shown in Fig. 6. Quite good agreement is found in this situation, confirming that the multiphase flow formulation can be used for droplet impingement calculation. In particular, the impingement limits are more accurately captured by the multiphase formulation, since the other methods are purely advective and the flow near the cylinder is highly elliptical. So, the diffusive terms of the multiphase approach make he difference in these cases.

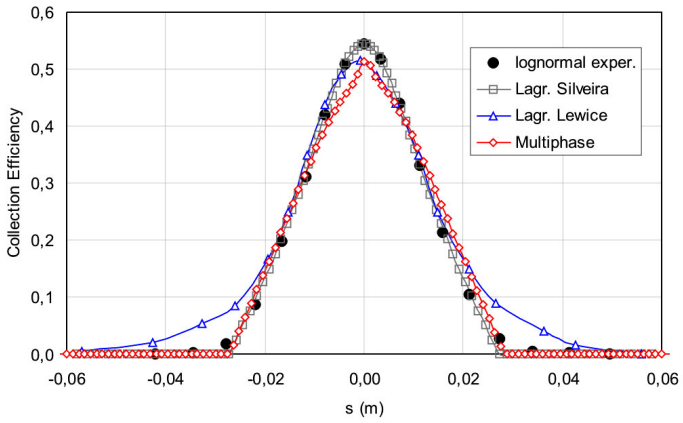

Figure 5: collection efficiency for NACA0012

The following figures show a series of results of the Lagrangean and Eulerian simulations. In Fig. 7 it can be seen the water droplets trajectories for the airfoil case. It can be noted a large number of trajectories passing near the impingement limits. This happens due to the searching process for the impingement limit locations.

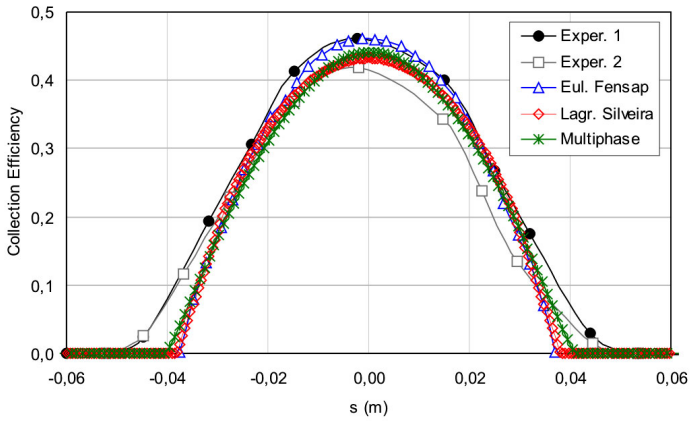

Figure 6: collection efficiency for the cylinder case

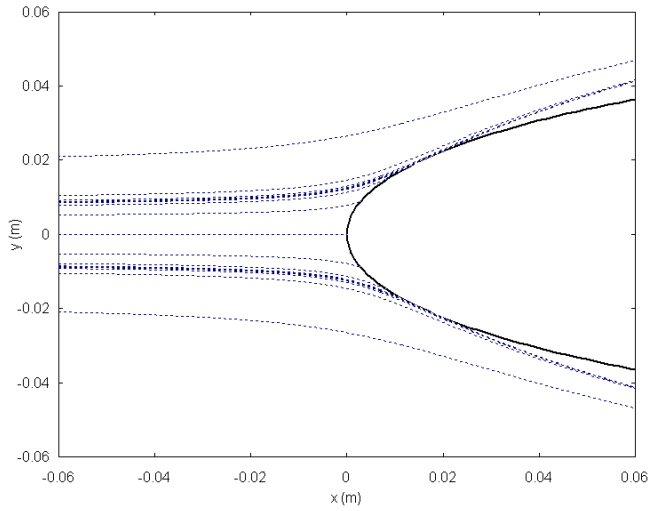

Figure 7: Impingement trajectories.

Figure 8 shows the trajectories calculated for the cylinder case. This case is computationally more expensive that the airfoil case, since the deviation of the trajectories is greater, requiring a large amount of computation for the water positions near the body, besides a smaller time step for accuracy and convergence.

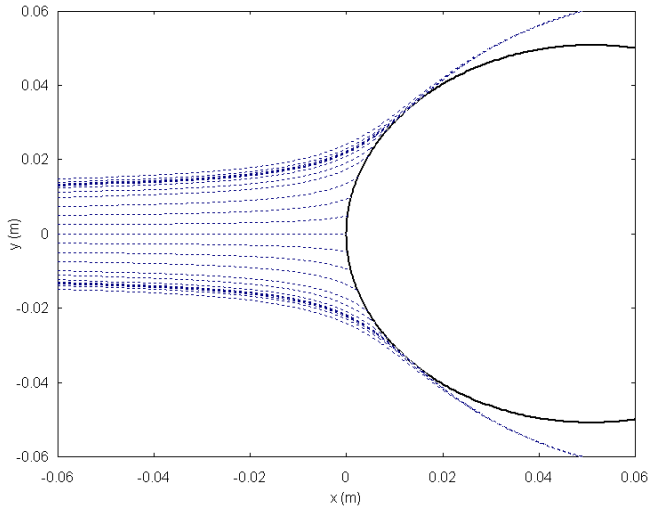

Figure 8: trajectories for the cylinder case.

The next figures show the results of the Eulerian simulation for the NACA0012 airfoil. The grid was created in the mesh generator ICEM CFD (Ansys Inc.) and contains about 50000 elements. A typical “C-mesh” used for the simulations in this paper is shown in Fig. 9.

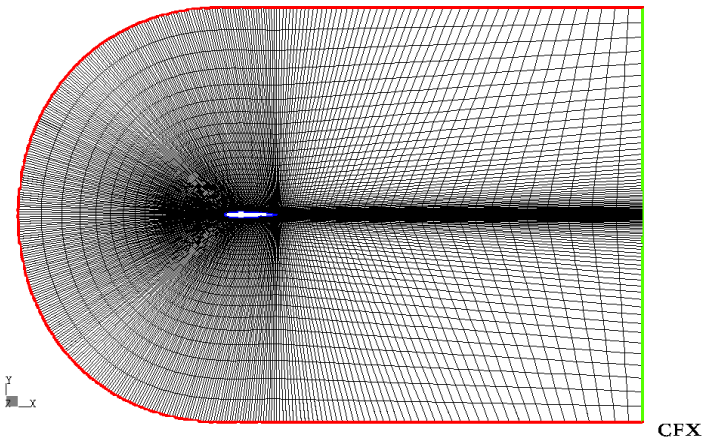

Figure 9: Grid for multiphase simulation.

The water volume fraction field is presented in Fig. 10. It can be observed the water accumulation in the region near the leading edge of the airfoil. The region over and above the body where the volume fraction is almost zero is known as the “shadow area”, since any water droplet is presented in those locations.

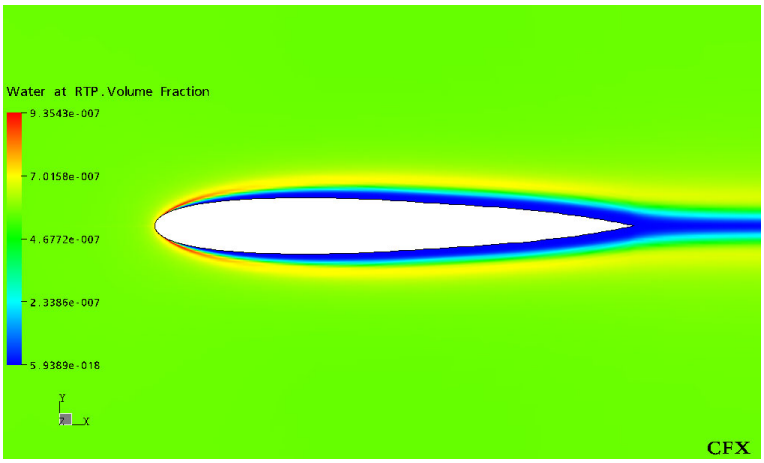

Figure 10: Water volume fraction contours for NACA 0012 airfoil.

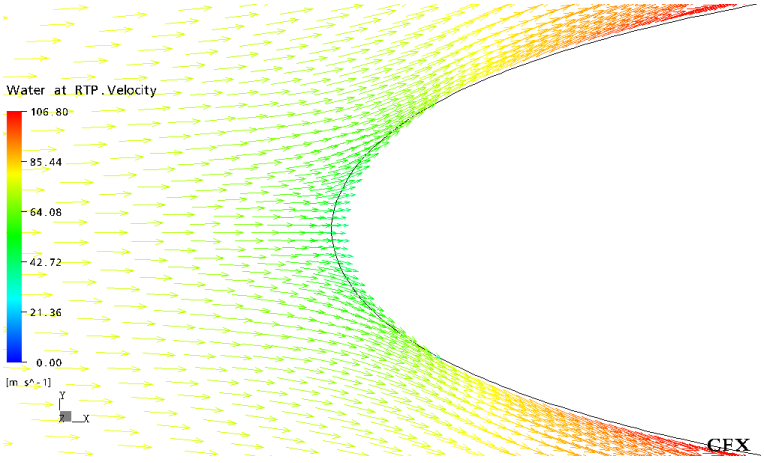

Figure 11: Velocity field for dispersed phase.

Finally, the water velocity vectors near the leading edge of the airfoil are presented. In Fig. 11, one can see the vectors “entering” the airfoil. Actually, they are leaving the domain, since the “interior” of the airfoil is an external region of the domain. The vectors lying just at the wall boundary are the impingement velocities that are required for the collection efficiency calculation.

5. Concluding Remarks

In this paper it was presented three different approaches for computing collection efficiency for icing analysis. The first and second formulations described in this work are well-known methodologies and they have been extensively used in the icing codes. It was shown that Lagrangean methods are more appropriate for simple two-dimensional geometries, since it is computationally cost-effective for such situations. For complex three dimensional geometries, two problems arise: one related to the impingement position determination and another to the air velocity interpolations that are required for the droplet positions. When using the Panel method for potential flow, the problem is on the number of operations required for computing the air velocity in some location when the number of points defining the geometry increases. The first Eulerian approach described is more applicable to complex geometries, as pointed out. However, some important effects are still not accounted for in this method, such the influence of the droplets in the air flow when the diameter increases, or the heat and mass transfer between the two phases, which may occur in special situations.

In order to capture the maximum number of possible physical effects, it was proposed an alternative approach for air-water droplets flow simulation. The multiphase model implemented in the software CFX contains a wide range of options, since it is a general model that can be used for a large number of physical problems. It was seen that particle induced turbulence can be considered with this model and it is very important effect when a large droplets distribution is present. Turbulence models for both air and water phases can be used and interphase heat and mass transfer can be accounted for other effects than drag.

It is expected that this work opens new possibilities of improving the existing icing codes. Since these are preliminary results, the multiphase formulation needs further analysis in order to extract as much as possible from its model.

6. References

AEA Technology plc., 2001, "CFX 5 Solver and Solver Manager Manual - Mathematical Models - Multihpase Flow".

Bourgault, Y., Habashi, W.G., Dompierre, J. and Baruzzi, G.S., 1999, "A Fininte Element Method Study of Eulerian Droplets Impingement Models", International Journal for Numerical Methods in Fluids, Vol. 29, pp. 429-449.

Bourgault, Y., Beaugendre, H. and Habashi, W.G., 2000 a, "Development of a Shallow Water Model in FENSAP-ICE", Journal of Aircraft, Vol. 37, No. 4, pp. 640-646

Bourgault, Y., Boutanios, Z. and Habashi, W.G., 2000 b, "Three-Dimensional Eulerian Approach to Droplet Impingement Simulation using FENSAP-ICE, Part 1: Model, Alorithm and Validation", Journal of Aircraft, Vol. 37, No. 1, pp. 95-103.

Gent, R.W., Dart, N.P. and Cansdale, J.T., 2000, "Aircraft Icing", Phil. Trans. R. Soc. Lond. A 358, pp. 2873-2911.

Wright, W.B., 1995, "Users Manual for the Improved NASA Lewis Ice Accretion Code Lewice 1.6", NASA CR – 198355.

Hedde, T. and Guffond, D., 1995, "ONERA Three-Dimensional Icing Code", AIAA Journal, Vol. 33, No. 6, pp.1038-1045.

Kind, R.J., Potapczuk, M.G., Feo, A., Golia, C. and Shah, A.D., 1998, "Experimental and Computational Simulation of in-Flight Icing Phenomena", Progress in Aeronautical Sciences, Vol. 34, pp. 257-345.

Messinger, B.L., 1953, "Equilibrium Temperature of an Unheated Icing Surface as a Function of Air Speed", Journal of Aeronautical Sciences, pp. 29-42.

Morency, F., Tesok, F. and Paraschivoiu, I., 1999, "Anti-Icing System Simulation using CANICE", Journal of Aircraft, Vol. 36, No. 6, pp. 999-1006.

Silveira, R. A., 2001 "Simulação Numérica da Fomrção de Gelo na Borda de Ataque de Perfis Aerodinâmicos", MsC Thesis, Federal University of Santa Catarina, Florianópolis, SC, Brazil, In Portuguese.

Silveira, R.A, Maliska, C.R, 2001, Numerical Simulation of Ice Accretion on the Leading Edge of Aerodynamic Profilies", Proceedings of the 2nd International Conference on Computational Heat and Mass Transfer, Rio de Janeiro, RJ, Brazil.